ACS OMEGA

http://pubs.acs.org/journal/acsodf

Article

Tetraphenylethene-Based Fluorescent Chemosensor with Mechanochromic and Aggregation-Induced Emission (AIE) Properties for the Selective and Sensitive Detection of Hg^{2+} and Ag^{+} Ions in Aqueous Media: Application to Environmental Analysis

Kishor S. Jagadhane, Sneha R. Bhosale, Datta B. Gunjal, Omkar S. Nille, Govind B. Kolekar, Sanjay S. Kolekar, Tukaram D. Dongale, and Prashant V. Anbhule*

Cite This: *ACS Omega* 2022, 7, 34888−34900

Read Online

ACCESS | Metrics & More | Article Recommendations | Supporting Information

ABSTRACT: It is critical to design a novel and simple bifunctional sensor for the selective and sensitive detection of ions in an aqueous media in environmental samples. As a result, in this study, tetraphenylethene hydrazinecarbothioamide (TPE-PVA), known as probe 1, was successfully synthesized and characterized as having impressive photophysical phenomena such as aggregation-induced emission (AIE) and mechanochromic properties by applying mechanical force to the solid of probe 1. The emission of the solid of probe 1 changed from turquoise blue to lemon yellow after grinding, from lemon yellow to parakeet green after annealing at 160 °C, and to arctic blue after fuming with DCM. Such characteristics could lead to a variety of applications in several fields. The probe was implemented and demonstrated remarkable selectivity and sensitivity toward mercury(II) and silver(I) ions by substantially switching off emission over other cations. Following an extensive photophysical analysis, it was discovered that detection limits (LOD) as low as 0.18344 and 0.2384 $\mu g\ mL^{-1}$ for Hg^{2+} and Ag^{+}, respectively, are possible with a quantum yield (Φ) of 2.26. Probe 1 was also explored as a Hg^{2+} and Ag^{+} paper strip-based sensor and kit for practical use. The binding mechanisms of probe 1 (TPE-PVA) with Hg^{2+} and Ag^{+} were confirmed by ^{1}H NMR titration. These results could lead to the development of reliable onsite Hg^{2+} and Ag^{+} fluorescent probes in the future.

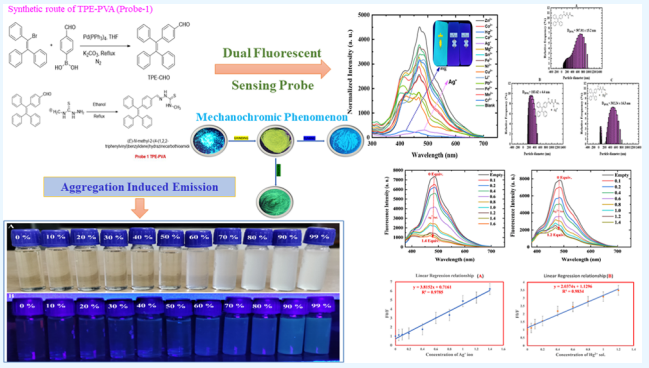

1. INTRODUCTION

Tetraphenylethylene (TPE)-based device materials have been of great interest in recent years for detecting metal ions in biological and environmental systems because of their aggregation-induced emission (AIE) properties,[1] high selectivity, sensitivity, and ease of evaluation. Tetraphenylethene is also a common building block for AIE photophysical phenomena. A carbothioamide derivative based on tetraphenylethene may exhibit AIE. Whenever illuminated with 365 nm ultraviolet (UV) light, dilute tetrahydrofuran (THF) solution of TPE-PVA emitted a modest yellowish color, whereas its solid emitted a strong yellowish color. Because of the hydrophobic nature of TPE, it is universally acknowledged that AIE-active sensors can be developed from TPE.[2] Aggregation-induced emission (AIE) compounds have a propeller-shaped structure, wherein $\pi-\pi$ stacking in aggregates and solids is avoided. Because of the hydrophobic characteristics of TPE, TPE-derived probes have long been recognized to be AIE-active.[3] Tetraphenylethylene has a propeller-shaped structure with rotating aromatic phenyl rings on the periphery. Recent research has discovered and proven that when in dilute solutions, free rotation of the peripheral aromatic rings is allowed. Nonradiative disintegration (decay) is induced by the excited state.[4] As a result of their "aggregation-induced emission" properties, tetraphenylethylene derivatives are the most commonly used chromophores to explain complexation with metal ions. The functionalization of the tetraphenylethylene-based molecular architecture with pendant coordinating sites for metal ions is a way of developing novel chemosensors for metal ion detection.[5] The AIE characteristics of tetraphenylethylene, which are based on the interaction of chromophore receptor sites with analytes, determine the detection capability of the compound.[6]

Recently, tetraphenylethylene and other aggregation-induced emission derivatives were successful in detecting Hg^{2+}

Received: June 2, 2022
Accepted: July 27, 2022
Published: September 21, 2022

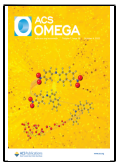

and Ag^+ ions in an aqueous medium as dual sensors.[7] It is worth noting that chromophores attached to methylene hydrazine carbothioamide have also sparked a lot of attention because of their high interaction abilities for transition metal ions in recent years.[8] However, methylene hydrazine carbothioamide-attached chromophores for metal ion sensing are infrequently studied, which surprised and motivated us to use them for the quantification of metal ions.[9] The major purpose of our research is to analyze the interaction and detection of all of these features, which have been used to create methylene hydrazine carbothioamide-attached TPE-based sensors with metal ions.[10,11]

Because of their high toxicity, heavy metals and transition ions have considerable harmful effects on the environment and human health, making selective and sensitive detection and quantification in biological, chemical, therapeutic, and environmental samples extremely vital. Mercury is an extremely harmful, nonbiodegradable heavy metal found across the world due to pollution.[12] Mercury ions (Hg^{2+}) are widely distributed in ecological systems such as air, water, and soil due to oil refining, mining, as well as fossil fuel combustion. By the action of microbes, organic mercury, including methylmercury, can be converted between elemental mercury and inorganic mercury ions inside the environment, which pass through the food chain and accumulate in the human body.[13] Hg^{2+} has a tremendous capacity to interact with biological ligands in vivo, which means that an overabundance of Hg^{2+} in the body can cause significant heart problems and a variety of irreversible illnesses related to the stomach, kidneys, and brain, including the central nervous system.[14,15] Hg^{2+} levels in drinking water must be lower than 6 parts per billion according to the WHO (30 nM). As a result, identifying Hg^{2+} in environmental, nutritional, and biological samples requires a sensitive, speedy, and reliable analytical technique.[16−19]

In addition to mercury, the widespread use of silver has also led to the continuous discharge of metallic Ag and silver ion (Ag^+)-containing effluents into the environment from industries and other sources, which affects our daily lives (e.g., antibacterial agents, catalysts, electronics, photography, and jewelry).[20] Ag^+ ions are incredibly harmful to humans, making them one of the most damaging heavy metal contaminants. By binding to thiol, amino, and carboxyl groups in enzymatic reactions and/or displacing other crucial metallic ions, Ag^+ ions can inactivate enzymes and cause considerable instability in biological systems. The correspondingly high quantity of Ag^+ ions in potable water systems, according to the Environmental Protection Agency's (EPA) Secondary Potable Water Standards, is 0.1 μg mL^{-1} (or 0.93 M). As a consequence, sensitive analytical methods for precisely recognizing trace Ag^+ ions are significant for water quality management, public health, and environmental control.[21,22]

Recently, inductively coupled plasma mass spectrometry, atomic absorption spectrometry, gas chromatography, and high-performance liquid chromatography have been used to detect Hg^{2+} and Ag^+ ions.[23] Unfortunately, because of the increasing equipment costs, sophisticated procedure processes, and skilled supervision, the widespread use of the traditional methods mentioned above has been limited. Fluorescent probe technologies provide significant advantages over these advanced systems for Hg^{2+} and Ag^+ detection, along with excellent sensitivity, high selectivity, ease of operation, low cost, and real-time sensing. In recent literature, several fluorescent probes are often used to monitor environmental and biological samples for Hg^{2+} and Ag^+ ions.[23] However, these luminous probes have some disadvantages, such as low sensitivity and a high limit of detection (LOD), which limits their practical applicability. As a result of the aforementioned challenges, as well as the prospective application of luminous chromophores, the development of advanced and novel luminous probes with many more advantages in the domains of agricultural, environmental, and biological studies remains promising and significant. In addition, there are no reports on the detection of both metal ions using a single fluorescent probe.[6,24]

Therefore, in this study, we present a novel dual-sensor probe 1 known as TPE-PVA having a quantum yield (Φ) of 2.26 with a pendant methylene hydrazine carbothioamide receptor region.[25] In a mixed aqueous medium (ACN: H_2O: 1:9, v/v), it was ultimately employed as a dual-sensor chemosensor for the selective and sensitive detection of Hg^{2+} and Ag^+ over other metal ions.[26] In contrast to previously described chemosensors, the sensing of Hg^{2+} and Ag^+ ions by probe 1 is based on the fluorescence "switch-off" mechanism. This type of mechanism is due to the static type of quenching. We also constructed a test strip by fabricating a probe 1 strip with Whatman filter paper for the successful onsite detection of Hg^{2+} and Ag^+ ions for real-world application to environmental analysis.

2. EXPERIMENTAL SECTION

2.1. Chemicals and Equipment. All chemicals were used as received from commercial suppliers, without further purification. The compound probe 1, known as TPE-PVA, was synthesized by reacting 4-(1,2,2-triphenylvinyl) benzaldehyde and 4-methyl-3-thiosemicarbazide in the presence of ethanol and acetic acid as solvents. The reagents required to synthesize probe 1 were procured from Sigma-Aldrich. The various cations of chloride, nitrate, and sulfate salts (such as Zn^{2+}, Co^{2+}, Hg^{2+}, Ca^{2+}, Ag^+, Mg^{2+}, Sn^{2+}, Fe^{3+}, Ni^{2+}, Cu^{2+}, Li^+, Pb^{2+}, Fe^{2+}, Mn^{2+}, Cr^{6+}, etc.) and DMSO were also purchased from Sigma-Aldrich and TCI.

Synthesized AIE luminogens were characterized by different characterization techniques such as infrared (IR) attenuated total reflection (ATR), ^1H NMR, and ^{13}C NMR spectroscopies and high-resolution mass spectrometry (HRMS). IR spectra were recorded on a Bruker, Germany (α), spectrometer in the range of 4000−400 cm^{-1}. ^1H NMR spectra were recorded on a 400 MHz Bruker Advance spectrometer and ^{13}C NMR using 101 MHz spectrometers, with $CDCl_3$-d or DMSO-d_6 used as solvents (trimethyl silane as an internal standard). DEPT-135-NMR spectra were recorded on a 400 MHz Bruker Advance spectrometer. Mass spectrometry (HR-MS) data were obtained using Waters Micromass Q-Tof Micro under the electrospray ionization (ESI)−MS mode. UV−vis absorption spectra were recorded by the Specord plus UV−vis double-beam spectrophotometer (Analytik Jena), and the fluorescence emission was measured on an FP-8300 (Jasco) fluorescence spectrometer. TLC (on a silica-coated aluminum plate) was used to monitor the progression of all of the reactions.

2.2. Synthesis of TPE-PVA. *2.2.1. Synthesis of TPE-CHO 4-(1,2,2-Triphenylvinyl)benzaldehyde.* The synthetic route for TPE-CHO is highlighted in Scheme 1.

1-Bromo-1,2,2-triphenylethylene (335.24 mg, 1.0 mmol) as well as 4-formylphenylboronic acid (179.9 mg, 1.2 mmol), were dissolved in 20 mL of tetrahydrofuran solution and 7 mL of 2 M potassium carbonate aqueous solution. The entire

https://doi.org/10.1021/acsomega.2c03437
ACS Omega 2022, 7, 34888−34900

Scheme 1. Synthetic Route to TPE-CHO 4-(1,2,2-Triphenylvinyl)benzaldehyde

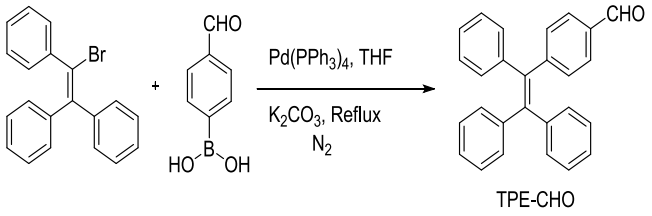

mixture was stirred for 0.5 h at room temperature under a nitrogen (N_2) atmosphere, then Tetrakis (triphenylphosphine) palladium(0) (0.010 g) was added, and the mixture was allowed to reflux at 80 °C overnight. TLC was used to monitor the progress of the reaction, and after it was completed, the solvent was removed under reduced pressure to form a residue. The formed residue was chromatographed on a silica gel column with *n*-hexane/dichloromethane (v/v 3:1) as an eluent to afford TPE-CHO as a light-yellow powder (346.0 mg, 96% yield).[27,28] ^{1}H NMR (400 MHz, $CDCl_3$) δ/ppm: 9.90 (s, 1H, −CHO), 7.62 (d, J = 8.5 Hz, 2H, −Ar−H), 7.20 (d, J = 8.3 Hz, 2H, −Ar−H), 7.15−7.09 (m, 9H, −Ar−H), 7.06−6.99 (m, 6H, −Ar−H). ^{13}C NMR: (101 MHz, $CDCl_3$) δ/ppm: 191.93, 150.56, 143.04, 142.99, 142.89, 139.74, 134.25, 131.95, 131.30, 131.28, 131.23, 129.17, 127.93, 127.74, 127.05, 126.89, 126.86, 124.46. HR−ESI−MS calculated for $C_{27}H_{20}O$ $[M + H]^+$: 361.1548; found: 361.1546. IR (ATR): 691, 1018, 1210, 1554, 1691, 2724, 2824, 3050, cm^{-1}; the structure of probe 1 was confirmed using a combination of characterization techniques, including IR, ^{1}H NMR, and ^{13}C NMR spectroscopies and HR-MS spectrometry.

2.2.2. Synthesis of the Desired (E)-N-Methyl-2-(4-(1,2,2-triphenylvinyl)benzylidene) Hydrazinecarbothioamide. The synthetic route of TPE-PVA is highlighted in Scheme 2.

Scheme 2 highlights the synthetic route for (*E*)-methyl-2-(4-(1,2,2-triphenyl)benzylidene) hydrazinecarbothioamide. 4-Methyl-3-thiosemicarbazide was dissolved in 10 mL of ethanol. Then, to this solution, 4-methyl-3-thiosemicarbazide and 1 mL of acetic acid were added. After that, the whole solution was refluxed at 80 °C for 30 min. On cooling to room temperature, the pale-yellow solute was deposited. TLC confirmed the completion of the reaction, and the final pale-yellow product was subsequently purified by column chromatography with petroleum ether/ethyl acetate (v/v = 30/1), yielding (*E*)-methyl-2-(4-(1,2,2-triphenylvinyl)benzylidene) hydrazinecarbothioamide (147.0 mg, 66% yield).[29] ^{1}H NMR (400 MHz, $CDCl_3$) δ/ppm: 9.56 (s, 1H), 7.72 (s, 1H), 7.37 (d, J = 8.5 Hz, 2H), 7.11 (qd, J = 3.9, 1.8 Hz, 9H), 7.07 − 7.00 (m, 9H), 3.23 (d, J = 4.9 Hz, 3H). ^{13}C NMR: (101 MHz, CDCl3) δ/ppm: 178.15, 146.32, 143.38, 143.34, 143.20, 142.26, 142.05, 140.05, 131.85, 131.34, 131.32, 131.27, 131.14, 127.85, 127.81, 127.69, 126.77, 126.69, 126.65, 31.15, 29.71, 29.37. IR (ATR): 691, 748, 818, 1022, 1080, 1249, 1546, 1691, 2853, 2924, 3624, 3742, cm^{-1}; HR−ESI−MS calculated for $C_{29}H_{25}N_3S$ $[M + H]^+$: 448.1803; found: 448.1895. Different characterization techniques, such as IR, ^{1}H NMR, and ^{13}C NMR spectroscopies, and HR-MS spectrometry, were used to confirm the structure of probe 1.

2.3. UV−Vis and Fluorescence Experiments. All stock solutions of cations (100 μg mL^{-1}) were prepared in double-distilled water by dissolving the appropriate quantity of metal salts in water. The stock solution of probe 1 (1×10^{-4} M) was prepared in acetonitrile. For spectral analyses, test solutions were prepared by mixing 1.0 mL (1×10^{-4} M) of probe 1 with 1.0 mL (100 μg mL^{-1}) of individual cations in a test tube, diluting to 10 mL with distilled water and allowing to stand for 10 min at room temperature, and then absorption and fluorescence (emission) spectra were recorded at room temperature.

2.4. Fluorescence Titration for the Detection of Hg^{2+} and Ag^+ Cations. Probe 1 (1 mL, 10^{-4} mol/L) in acetonitrile solution was placed in each test tube of the different sets, and a fraction of varying concentrations of the aqueous solution of Hg^{2+} and Ag^+ (1 ppm) ions was added. All solutions were diluted to a constant volume. Eventually, all test-tube solutions were subjected sequentially to absorption and emission measurements at room temperature. The fluorescence spectra were recorded at λ_{ex} = 270 nm with a bandwidth of 10.

2.5. Preparation of Probe 1 Paper Strips. The paper strips were obtained by cutting Whatman paper. The test strips were prepared by submerging them in an acetonitrile solution containing probe 1 (1×10^{-4}). The strips were dried in the open air. The purpose of these test strips was to detect Hg^{2+} and Ag^+ in the presence of other cations. The test strips were examined under UV irradiation at 365 nm and used for easy detection with the naked eye.

2.6. DLS Study. The probe solution was prepared in acetonitrile (1×10^{-4}); the water−mixture solution and the metal ion solution were prepared in double-distilled water. Dynamic light scattering (DLS) measurements were carried out with only a probe and then the same measurements were carried out in the presence of metal ion solutions of Hg^{2+} and Ag^+ in the ratio of 1:0.5.

3. RESULTS AND DISCUSSION

3.1. Characterization of TPE-PVA (Probe 1). The synthesis of probe 1 is represented in Scheme 2, and Section 2 describes the specifics of the synthesis. Physicochemical and

Scheme 2. Synthetic Route to (*E*)-*N*-Methyl-2-(4-(1,2,2-triphenylvinyl)benzylidene)Hydrazinecarbothioamide (TPE-PVA)

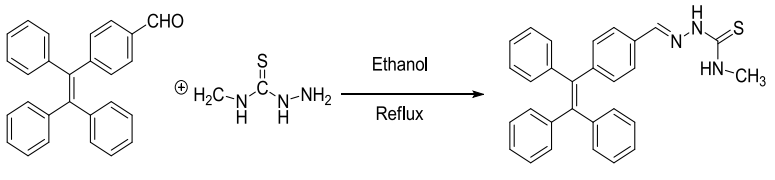

(*E*)-*N*-methyl-2-(4-(1,2,2-triphenylvinyl)benzylidene)hydrazinecarbothioamide

Probe 1 TPE-PVA

https://doi.org/10.1021/acsomega.2c03437
ACS Omega 2022, 7, 34888−34900

spectroscopic analyses were performed to describe it completely. To validate the purity and structure of the probe, FT-IR, ^{1}HNMR, ^{13}CNMR, and HR-MS spectra were obtained. This study revealed the successful synthesis of **TPE-PVA** (for more information, please see the Supporting Information).

3.2. AIE Properties. As a result, the solid powder of probe 1 emits bright yellow fluorescence. For the AIE study, we started by analyzing the emission spectra in different solvents such as THF and acetonitrile (ACN). The results are depicted in Figure 1C. In THF and acetonitrile (ACN), probe 1 showed fluorescence emission peaks at 420 and 426 nm in THF and ACN solvents, respectively, after excitation at 270 nm. In this study, we observed that probe 1 (TPE-PVA) shows a much weaker emission intensity compared with acetonitrile (ACN), and so THF solvent was selected for further AIE studies. According to the emission spectrum analysis, the solvent plays a major role, which seems to have a solvophobic effect.

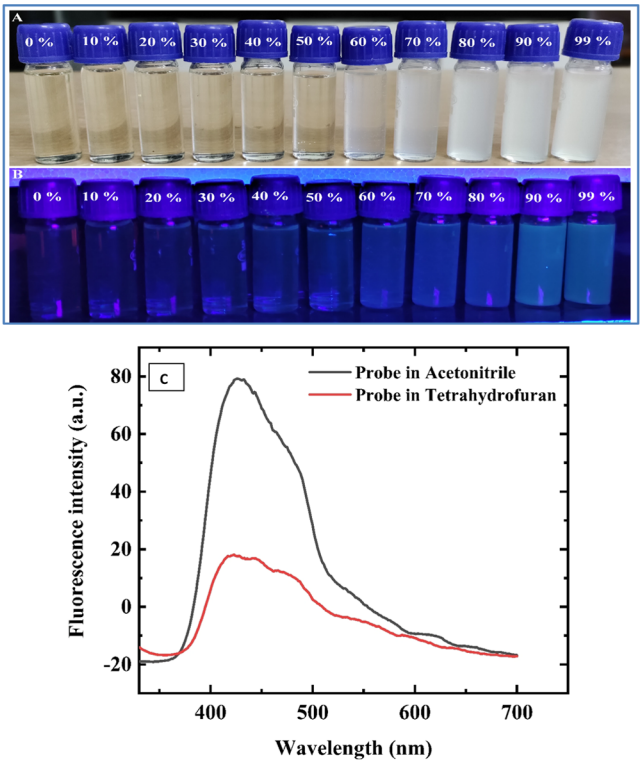

Figure 1. Images of aggregation-induced emission (AIE) in THF: H_2O mixtures with different water fractions (0−99%): (A) under daylight; (B) under UV (365 nm) irradiation; (C) probe in acetonitrile and tetrahydrofuran (10^{-6} M) for the AIE study.

In 2001, Tang and his group came up with the concept of aggregation-induced emission (AIE), which is a kind of photophysical phenomenon linked to the aggregation of the chromophore moiety.[30] In an aggregation-induced emission (AIE) process, weak or nonemissive luminogens become emissive due to the formation of their aggregates, which depends on the quantity of water in the mixture. These remarkably fluorescent luminogens, or AIEgens, are widely used interesting materials in diverse fields.[31−37]

The synthesized TPE-PVA was soluble in THF but insoluble in water. Therefore, by varying the water percentage in THF, the AIE property of TPE-PVA (10^{-3} M) was examined, and the results are shown in Figure 1. It was discovered that TPE-PVA aggregation begins in THF/H_2O combinations when the water content is 60% or greater. The TPE-PVA compound emits a modest fluorescence at 466 nm in a dilute THF solution and remains constant when the amount of water is increased from 0 to 70%. When water fractions (fw) in a solution approach 70%, the emission band centered at 466 nm is rapidly turned on and the fluorescence intensity increases constantly with increasing fw. The photographic images obtained in daylight indicate that when 70−99% of water is added, the solution transforms from clear to turbid (Figure 1A). When the fw is greater than 70%, the same images under UV irradiation exhibited fluorescence, which increased with the fw (70−99%) (Figure 1B). TPE-PVA appears to be an AIE-active compound by this photographic analyses.[38]

The AIE properties of TPE-PVA were further studied by fluorescence measurement. Figure 2A depicts the fluorescence emission spectra of solutions with different water fractions. In the THF solution, probe 1 (TPE-PVA) produced an extremely weak emission band at 431 nm after excitation at 270 nm (Figure 2A, black line). The addition of water (up to 60%) to the TPE-PVA solution led to a gradual increase in the fluorescence intensity. As soon as the water fraction reached 70%, there was a modest increase in the emission intensity.

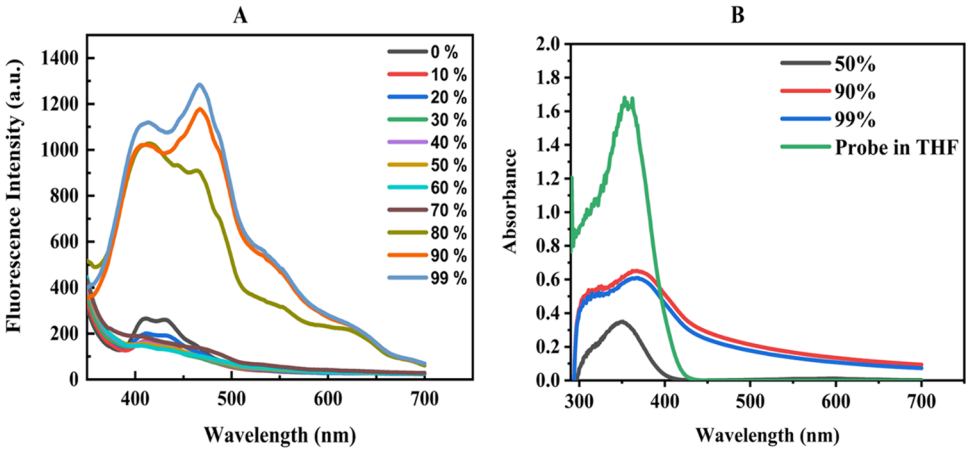

Figure 2. (A) Emission spectra (PL) of probe 1 (TPE-PVA) in THF/H_2O (v/v) mixtures with different water fractions were recorded at λ_{ex} = 270 nm. (B) Absorption spectra (UV−vis) of probe 1 (TPE-PVA) in THF and THF/H_2O fw.

https://doi.org/10.1021/acsomega.2c03437
ACS Omega 2022, 7, 34888−34900

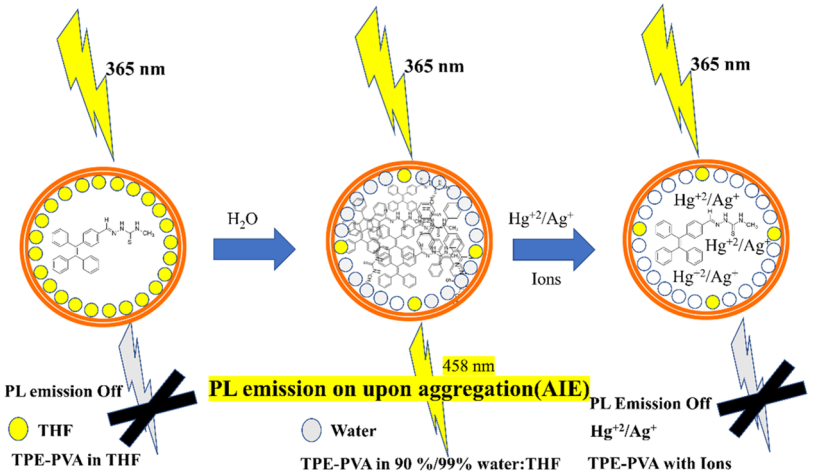

Figure 3. Schematic Representation of Investigations of the Fluorescent On/Off Emission Depending on AIE for the Detection of Metal Ions Hg^{2+}/Ag^{+}.

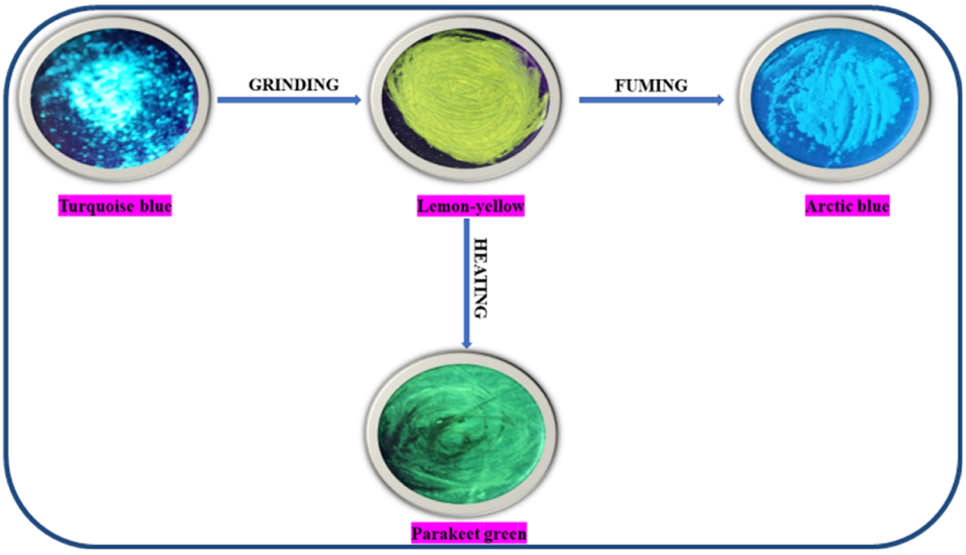

Figure 4. Under UV irradiation (365 nm), images exhibiting the mechanochromic phenomenon of probe 1 show color changes after grinding, fuming, and heating.

The fluorescence intensity of probe 1 suddenly increased as the proportion of water in the THF solution was increased to 80, 90, and 99% (Figure 2A). A substantial fluorescence intensity boost was found in the THF solution of probe 1 at 99% water fraction (Figure 2A, faint blue line).[39]

In the aggregated state, constricted molecular packaging restricts the intramolecular rotation vibrations of the molecules, which results in the strengthening of the π-conjugation of TPE-PVA molecules. As a result, only radiative decay is possible; hence, AIE is observed in the aggregated state. In contrast, the TPE-PVA moiety is essentially isolated in a THF medium and has limited contact with other TPE-PVA molecules. Therefore, there is less dense packaging of molecules. As a result, TPE-PVA in THF solution shows negligible emission because the major nonradiative decay is caused by free rotation and vibrational modes. The formation of TPE-PVA molecular aggregates with the addition of water is ascertained by fluorescence and absorption measurements in a THF/H_2O solvent mixture with various water fractions. The feeble emission band of TPE-PVA compounds in THF was centered at 409 nm in the emission spectra. On increasing the water content from 70 to 99%, the previous band disappeared and a new emission peak at 466 nm was observed (Figure 17a). This shift with an increase in the fluorescence is due to the aggregation of TPE-PVA molecules (Figure 2A).[40]

The UV−visible absorbance spectra of probe 1 in tetrahydrofuran only and in a different mixture of THF and H_2O are presented in Figure 2B. Probe 1 has an absorbance maximum of 358 nm in THF. Probe 1 shows a marked change in the absorption peak, observed at 368 nm with a 10 nm shift, which is a red shift after being added to 99% water. This implies that probe 1 undergoes J-aggregation due to the presence of water. All of the obtained results confirmed that probe 1 had outstanding AIE properties and had the maximum fluorescence intensity in THF/H_2O (fw = 99%). In the realm of fluorescence probes, the AIE behavior of TPE-PVA is unique.

A detailed schematic diagram presents the investigation of the fluorescent on/off emission based on AIE (aggregation-induced emission) for the detection of metal ions, particularly Hg^{2+}/Ag^{+}. In general, the synthesized probe has zero or low emission in an organic solvent (THF); after an increase in the

https://doi.org/10.1021/acsomega.2c03437
ACS Omega 2022, 7, 34888−34900

quantity of a poor solvent (water), PL emission increases following the formation of an aggregate as a result of the aggregation-induced emission of the synthesized probe. We discovered that after adding an analyte solution to aqueous media, the PL emissions of Hg^{2+} and Ag^{+} were turned off selectively. The detailed schematic illustration is displayed in Figure 3.

3.3. Mechanochromic Properties. Mechanochromic luminescence (MC) is a unique property of some smart materials and molecules, which occurs in response to mechanical forces such as grinding, heating, fuming, and crushing/rubbing.[41] The MC luminescence characteristic has garnered much attention because of its potential uses in mechanosensory applications, security papers, and optical storage.[42] The mechanochromic aspects of probe 1 in its solid state were investigated due to the aggregation-induced emission (AIE) nature of TPE-PVA. A mortar and pestle were used to grind probe 1 (TPE-PVA) to determine its mechanochromic luminescence response. The color of the grounded TPE-PVA under UV light (365 nm) is shown in Figure 4 accordingly. The emission color of probe 1 changed drastically when the solid sample was ground with a pestle and mortar; the original turquoise blue emission turned into a lemon yellow color. Moreover, annealing and fuming with the vapor of the solvent also influenced the color of probe 1 in its solid state. Probe 1 changed its color from lemon yellow to parakeet green and arctic blue after annealing at 160 °C and fuming with dichloromethane (DCM), respectively (Figure 4).

Further, the mechanochromic properties of probe 1 (TPE-PVA) were supported by powder X-ray diffraction (PXRD) patterns.[43] The PXRD pattern was obtained before grinding (Figure 5I). This pattern shows several sharp peaks (between

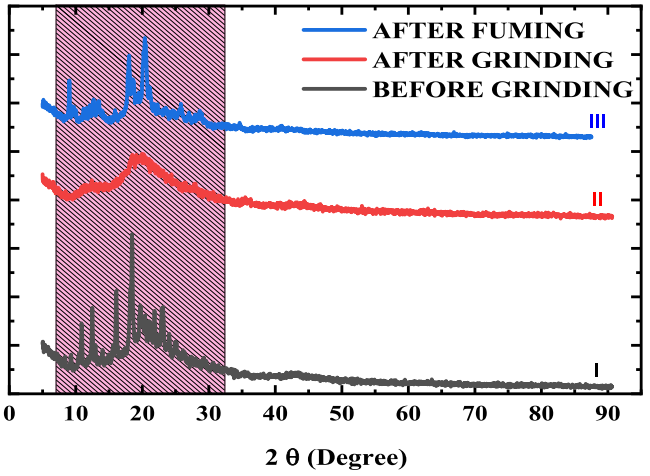

Figure 5. AIE luminogen probe 1 (TPE-PVA) XRD patterns in various solid states (I, original; II, ground; and III, fuming).

2θ = 10 and 25°) along with a broadened peak at 2θ = 20° (in the range of 2θ = 16−35°). This broad peak corresponds to the (101) plane of carbonaceous materials containing N and S heteroatoms. In addition, one more broad peak was observed at 2θ = 42.5°, related to the (034) plane, and it is well-matched to JCPDS card no. 01-078-1129. All of these factors confirmed the monoclinic phase of probe 1 before grinding (space group = *P21/n*, space group no. = 14).

Further, after grinding the powder of probe 1 with a mortar and pestle for 2 min, all sharp peaks disappeared and only broad peaks were observed at 2θ = 12.5 and 20°. This indicated the completely amorphous nature of the compound (Figure 5II). Again, TPE-PVA was subjected to annealing and fuming to determine whether it reverted to its original state or not. Therefore, the PXRD pattern after fuming with dichloromethane was recorded, which showed many more sharp diffraction peaks in the spectrum compared with its previous state, indicating the acquisition of a crystalline state. However, peak positions revealed that it did not revert entirely to its original crystalline state (before grinding) (Figure 5III). Hence, the transformation between the crystalline and amorphous phases of probe 1 (TPE-PVA) after grinding was accountable for its mechanochromic luminescence phenomenon.[44,45]

3.4. Fluorescence Response of Probe 1 to Various Cations. The metal recognition properties of probe 1 (TPE-PVA) were investigated by fluorescence as well as UV−vis spectroscopies. A 1×10^{-5} M solution of probe 1 in acetonitrile was studied in the presence of various biologically and environmentally important cations, such as Zn^{2+}, Co^{2+}, Hg^{2+}, Ca^{2+}, Ag^{+}, Mg^{2+}, Sn^{2+}, Fe^{3+}, Ni^{2+}, Cu^{2+}, Li^{+}, Pb^{2+}, Fe^{2+}, Mn^{2+}, Cr^{6+}, etc., in an aqueous medium. The emission spectra of the suspension of probe 1 exhibited the maximum emission at a wavelength of 466 nm when excited at 270 nm (Figure 17a,b). The addition of 100 μg mL^{-1} solutions of various cations to the probe 1 solution caused variations in the fluorescence emission spectra of probe 1. However, the fluorescence spectrum of probe 1 showed significant and drastic quenching of fluorescence in the presence of Hg^{2+} and Ag^{+} ions, indicating that probe 1 is suitable for the selective and sensitive detection of Hg^{2+} and Ag^{+} in mixed aqueous media. The results are depicted in Figure 6. Although the

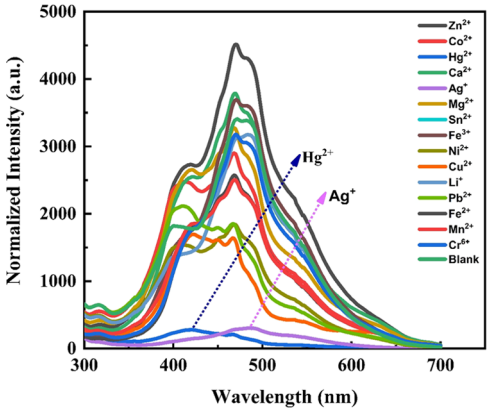

Figure 6. Emission spectra of probe 1 upon excitation at a wavelength of 270 nm. PL of probe 1 with the addition of various metal ions in a mixed (1:9, ACN: H_2O) aqueous medium.

mentioned cations decrease the fluorescence intensity, the decrease in fluorescence is negligible compared with that caused by Hg^{2+} and Ag^{+} ions. The remarkable thing in this fluorescence experiment is that the concentration of all of the cations is the same, which is prepared in double distilled water where Hg^{2+} and Ag^{+} ions flatten the curve completely compared with the rest of the cations. This reveals that Hg^{2+} and Ag^{+} ions have much more affinity compared with other tested cations.

Changes in fluorescence were also recorded under daylight and UV light, and the results are depicted in Figure 7A and B,

https://doi.org/10.1021/acsomega.2c03437
ACS Omega 2022, 7, 34888−34900

Figure 7. Solution of probe 1 in a mixed aqueous medium of ACN: H_2O (1:9 v/v): (A) under ambient light and (B) under UV irradiation (365 nm).

respectively. Under ambient light, probe 1 in mixed aqueous media (acetonitrile: water) with various cations showed less emission (Figure 7A), whereas under UV light, all tubes, except those containing Hg^{2+} and Ag^{+} ions, showed excellent fluorescence due to AIE (Figure 7B).

The diminished fluorescence of the probe 1 solution containing Hg^{2+} and Ag^{+} ions may be due to the interaction between the probe and ions. However, the other mentioned ions may not have interacted with probe 1; hence, there was no appreciable change in the fluorescence. These findings suggest that probe 1 (TPE-PVA) can selectively detect Hg^{2+} and Ag^{+} ions over the most relevant cations. As a result, probe 1 can be used as a fluorescent sensor for Hg^{2+} and Ag^{+} ions.

3.5. UV−Vis Absorption Study. The UV−vis spectra of the synthesized probe 1 (TPE-PVA) were recorded in acetonitrile: water mixed solvent at room temperature. The maximum absorption of the probe was centered at a wavelength of 362 nm. Figure 8 shows the UV−vis absorption spectra of probe 1 with the addition of each cation in an aqueous medium (ACN: H_2O 1:9 v/v).

Except for Hg^{2+} and Ag^{+} ions, the UV−vis absorption of probe 1 did not change significantly with the addition of the other tested cations. The absorption spectra changed drastically when the Hg^{2+} and Ag^{+} ions were added; the absorption maxima at 362 nm vanished completely, and a new band emerged at 352 nm. The complex formation of Hg^{2+} and Ag^{+} ions with probe 1 might be the reason for the appearance of new peaks or variations in UV−vis absorption spectra- (Figure 8). The appearance of a new absorption band at 350 nm for Hg^{2+} and at 354 nm for Ag^{+} is due to the complexation between Hg^{2+} and Ag^{+} and the organic moiety, respectively.

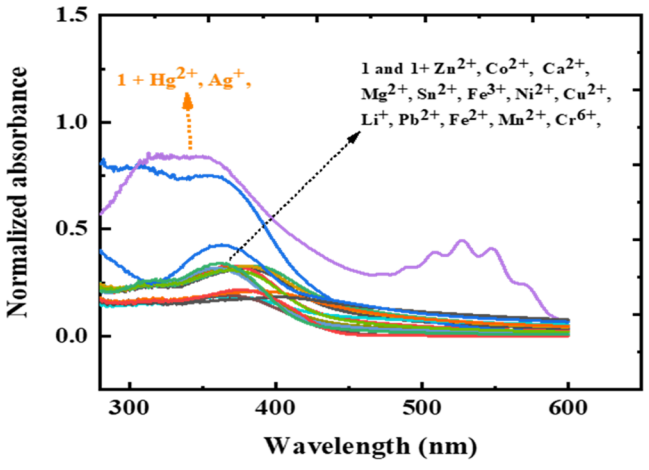

Figure 8. UV−vis absorption spectra of probe 1 (1×10^{-5} M) in the presence of Zn^{2+}, Co^{2+}, Hg^{2+}, Ca^{2+}, Ag^{+}, Mg^{2+}, Sn^{2+}, Fe^{3+}, Ni^{2+}, Cu^{2+}, Li^{+}, Pb^{2+}, Fe^{2+}, Mn^{2+}, and Cr^{6+} in a mixed aqueous medium of ACN: H_2O (1:9 v/v).

3.6. Fluorescence Sensing Performance. The sensing performance of probe 1 toward Hg^{2+} and Ag^{+} ions in a mixed aqueous medium (acetonitrile: water v/v 1:9) was investigated by fluorescence emission spectral analysis. The spectral results are depicted in Figure 9. A fluorescence emission band at 466 nm was observed in probe 1 in acetonitrile after excitation at 270 nm. The variations in the emission band at 466 nm were monitored with the addition of a series of different concentrations of Hg^{2+} and Ag^{+} ions in the probe 1 solution. With the gradually increasing addition of Hg^{2+} and Ag^{+} ions (0.1−1.6 μg mL^{-1}), the fluorescence of the probe 1 solution diminished, and it almost completely vanished after the addition of 1.6 μg mL^{-1} of both the ions (Figure 9A, B). Therefore, we speculated that the qualitative and quantitative determination of Hg^{2+} and Ag^{+} ions could be achieved easily with the developed organic probe.

To develop an analytical method for the quantification of analytes, there should be a linear association between the analyte concentration and the signal intensity.

Hence, to evaluate the analytical linear range, a standard Stern−Volmer quenching relationship was employed:

$$F_0/F = 1 + K_{SV}[Q] \quad (1)$$

where F_0 and F are the fluorescence intensities in the absence and presence of Ag^{+} and Hg^{2+} ions, respectively, K_{SV} is the Stern−Volmer constant, and [Q] is the concentration of ions.[46]

The plot of F_0/F vs the concentration of both the ions was plotted, which demonstrates a linear relationship between the fluorescence response and their concentration within the range of 0−1.4x and 0−1.2x μg mL^{-1} for both ions, respectively. Good linear regression coefficients (R^2) of 0.9785 and 0.9834 were obtained for Ag^{+} and Hg^{2+} ions, respectively (Figure 10).

3.7. Detection Limit. The limit of detection (LOD) of the developed method for both ions was evaluated subsequently using eq 2 (Haldar and Lee, 2018):[25]

https://doi.org/10.1021/acsomega.2c03437
ACS Omega 2022, 7, 34888−34900

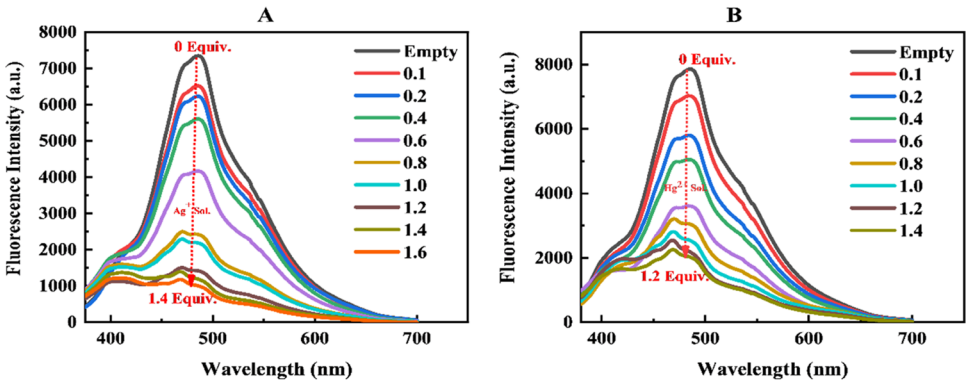

Figure 9. Addition of silver and mercury salt (aqueous) solutions to probe 1 solution: (A) Ag^+ (0−1.6 μg mL^{-1}) and (B) Hg^{2+} (0−1.4 μg mL^{-1}).

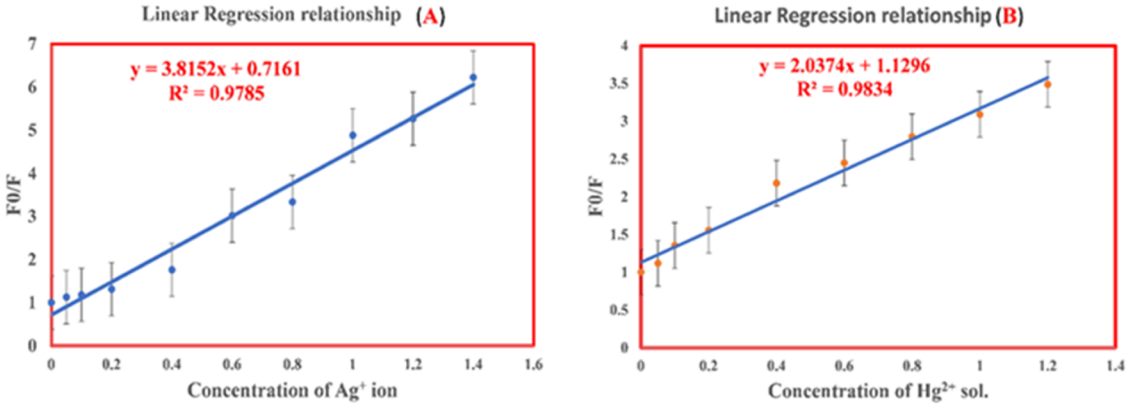

Figure 10. Linear regression relationship between the relative FL intensity and the concentration of (A) Ag^+ and (B) Hg^{2+} ions.

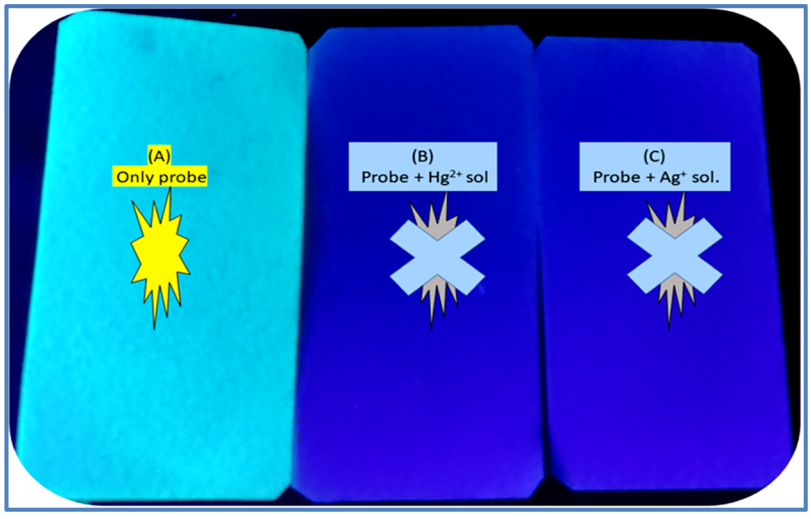

Figure 11. Images of paper strips loaded with probe 1 (TPE-PVA): (A) only probe; (B) probe 1 + Hg^{2+} solution; and (C) probe 1 + Ag^+ solution.

$$\text{detection limit} = 3\,\sigma/K \quad (2)$$

where K is the slope of the plot between the ratio of the emission intensity vs probe 1 and s is the standard deviation of the blank measurement, obtained using the Stern−Volmer plot; the LODs of the developed sensing system were found to be 0.18344 and 0.2384 μg mL^{-1} for Hg^{2+} and Ag^+ separately. These LODs are well below the permissible levels for both ions in drinking water. The obtained linearity, correlation coefficient, and LOD of the sensing system reveal its reasonable accuracy, making it a potential technology that might be studied for assaying both ions in actual samples.

3.8. Paper-Based Strips for the Onsite Detection of Hg^{2+} and Ag^+. The visual onsite screening of Hg^{2+} and Ag^+ ions was demonstrated using a paper-based strip. It was developed by soaking a paper strip in a probe 1 acetonitrile solution and then drying. Further, it was assayed for Hg^{2+} and Ag^+ ions and was observed under UV irradiation, as presented in Figure 13. It was observed that the probe 1 test paper exhibited a bright blue fluorescence under UV light (Figure 11A). The fluorescence of the paper strip test paper of probe 1

https://doi.org/10.1021/acsomega.2c03437
ACS Omega 2022, 7, 34888−34900

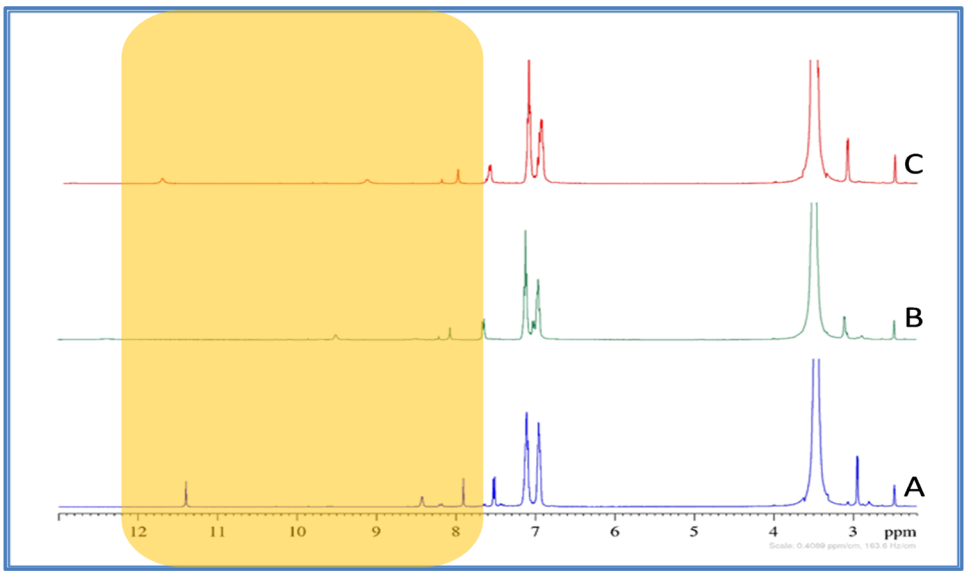

Figure 12. ^{1}H NMR spectrum of (A) only probe (TPE-PVA), (B) probe with Hg^{2+} (probe + Hg^{2+}), and (C) probe with the Ag^{+} (probe + Ag^{+}).

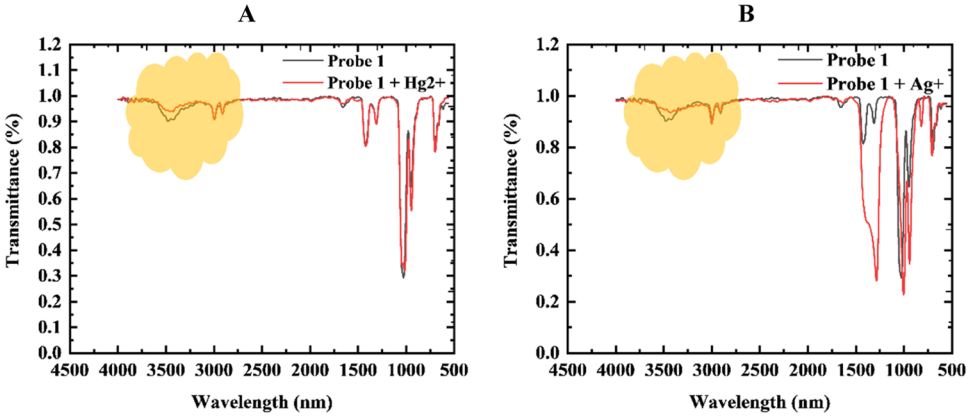

Figure 13. FT-IR spectra of probe 1 before and after the formation of a complex with (A) Hg^{2+} and (B) Ag^{+} ions.

diminished following the addition of Hg^{2+} and Ag^{+} ions under UV light (Figure 11), but competing cations had no effect (not shown here). These findings show that probe 1 may be used for the visual detection of Hg^{2+} and Ag^{+} ions with outstanding selectivity, sensitivity, stability, speed, and operational simplicity, without the need for complicated apparatus.

3.9. Sensing Mechanism. The TPE-PVA probe was assessed for the detection of Hg^{2+} and Ag^{+} ions sequentially by analyzing the decreases in the fluorescence intensity of the probe with the addition of ions. It was speculated that the complexation between the probe and ions might be responsible for the quenching of the fluorescence. Such a mechanism of sensing has been ascertained by different techniques as follows.

3.9.1. ^{1}H NMR. To confirm the mechanism of sensing for the Hg^{2+} and Ag^{+} ions with TPE-PVA, ^{1}H NMR experiments were performed in DMSO-d_6 because of the good solubility of probe 1 and salts ($HgCl_2$ and $AgNO_3$), which are illustrated in Figure 12. The ^{1}H NMR spectra of probe 1 demonstrated sharp peaks at δ_H 11.40 and 8.42 ppm, attributed to the NH proton. Upon the addition of Hg^{2+} and Ag^{+} ions ($HgCl_2$ and $AgNO_3$) to probe 1, the peaks that were observed at δ 11.40 and 8.42 ppm in 1H NMR of the probe gradually disappeared and shifted downfield (Figure 12A–C). Subsequently, this leads to an alteration in the original molecular architecture of probe 1. These results indicate that Hg^{2+} and Ag^{+} ions form a strong complex with the probe through the NH bond.[47]

3.9.2. FT-IR Spectrum. The FT-IR spectra of probe 1 (Figure 13) show peaks at 3450 (N–H stretching), 3000 (aromatic C–H stretching), 1650 (imine), and 1020 (C–N stretching) cm^{-1}. After the addition of Hg^{2+} and Ag^{+} ions in the probe solution, the N–H stretching peak at 3450 was weakened, whereas other peaks remained intact (Figure 13A, B). These results indicate that stable complex formation with ions occurs, confirming the involvement of N–H in the complexation process.[47]

3.9.3. DLS Study. Dynamic light scattering (DLS) was used to examine the aggregation of probe 1 solution with and without Ag^{+} and Hg^{2+} ions. A sample solution of the probe was prepared in ACN: H_2O (v/v, 1:9) for DLS measurements and showed a size distribution of 507.01 ± 15.2 nm in diameter (Figure 14A). The large size of probe 1 was due to their aggregation in mixed media. However, with the addition of Ag^{+} and Hg^{2+} ions to the probe solution, the size was reduced to 183.62 ± 4.4 nm (Figure 14B) and 302.24 ± 16.3 nm in diameter for Ag^{+} and Hg^{2+} ions, respectively (Figure 14C). The size reduction was attributed to the breakdown of aggregation of the probe due to the complex formation with Ag^{+} and Hg^{2+}, where probe 1 immediately compacted with

https://doi.org/10.1021/acsomega.2c03437
ACS Omega 2022, 7, 34888–34900

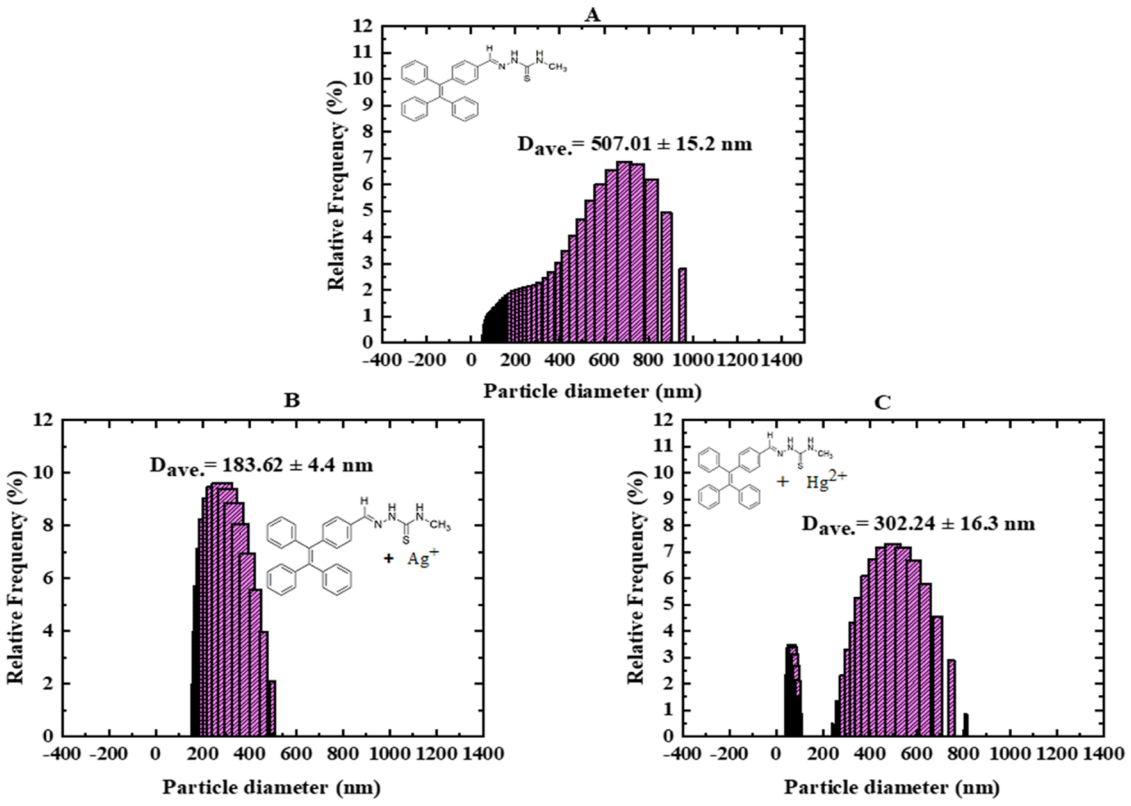

Figure 14. DLS data of probe 1 in the (A) absence and (B, C) presence of Ag^{+} and Hg^{2+} ions.

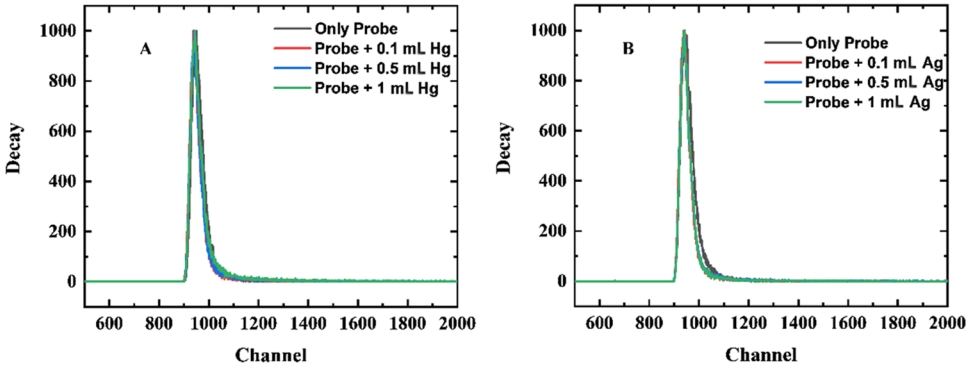

Figure 15. Fluorescence decay profile (lifetime) of probe 1 (TPE-PVA) in the absence and presence of different concentrations of metal ion solutions: (A) only probe and Hg^{2+} addition and (B) only probe and Ag^{+} addition.

ions to form smaller particles.[48,49] Thus, DLS data revealed that probe 1 readily forms complexes with Ag^{+} and Hg^{2+} ions.

3.9.4. Fluorescence Lifetime. Time-correlated single-photon counting (TCSPC) was also used to confirm the mechanism behind the selective sensing of Hg^{2+} and Ag^{+} over other metal ions in aqueous media. Either the electron transfer or complex formation mechanism might be primarily responsible for quenching the emission of probe 1 with Hg^{2+} and Ag^{+} ions. Measurement of the fluorescence lifetime is an effective tool to differentiate such quenching mechanisms. The decay times of probe 1 with increasing volumes (0.1, 0.5, and 1 mL) of Hg^{2+} (1 μg mL^{-1}) solution were recorded (Figure 15A). Similarly, the decay times of probe 1 with increasing volumes (0.1, 0.5, and 1 mL) of Ag^{+} (1 μg mL^{-1}) solution were also recorded (Figure 15B). If $\tau_0/\tau = F_0/F$, the type of quenching that occurs is dynamic, and if $\tau_0/\tau = 1$, the type of quenching that occurs is static, where τ_0 and τ_1 are the lifetimes of the fluorophore (probe 1) before and after the addition of the quencher (Hg^{2+} and Ag^{+}), respectively. The results revealed that $\tau_0/\tau \approx 1$, which indicates that a static form of quenching occurs between probe 1 and Hg^{2+} and Ag^{+} ions. Thus, complexation between the probe and ions occurs in the ground state.

3.9.5. Binding Constant and Binding Sites. Fluorescence quenching data at room temperature, i.e. 298 K, were used to calculate binding parameters such as the binding constant (K) as well as binding sites (n). The binding parameters were calculated using eq 3 given below:

$$\log[(F_0 - F)/F] = \log K + n \log[Q] \quad (3)$$

where K and n are the binding constant and the number of binding sites, respectively. The values of K and n were determined by plotting $\log[(F_0 - F)/F]$ against $\log[Q]$ at room temperature, as shown in Figure 16. The intercept and

https://doi.org/10.1021/acsomega.2c03437
ACS Omega 2022, 7, 34888−34900

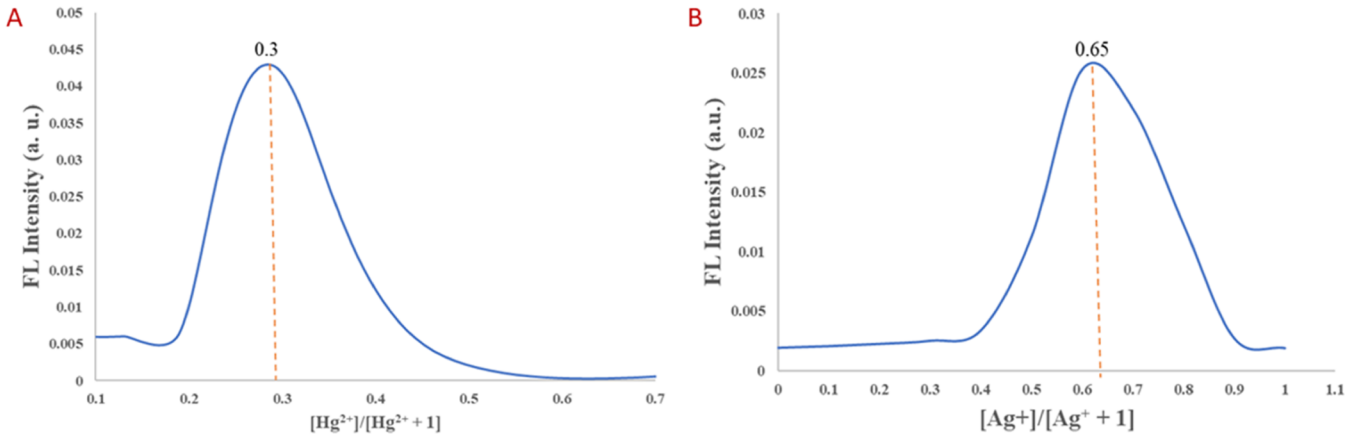

Figure 16. Job's plot for probe 1 association: (A) stoichiometric complexation of probe 1 with Hg^{2+}; (B) stoichiometric complexation of probe 1 with Ag^{+}.

slope, as well as the regression coefficient, were used to derive the binding constant (K) and binding sites (n). For probe 1 (TPE-PVA), the results demonstrate the presence of a single class of binding sites (n^a) approximately 1 (Table 1).

Table 1. Binding Constant (K) and Number of Binding Sites (n) Between Probe 1 and Analytes

analytes	binding constant K ($\times 10^6$ dm^3 mol^{-1})	number of binding sites (n^a)	correlation coefficient (R)
Hg^{2+}	0.08	0.90	0.98
Ag^{+}	3.41	1.20	0.97

3.9.6. Job's Plot. Using Job's plot (the method of continuous variation), the binding stoichiometry of the final complex between probe 1 and Ag^{+} was determined, which is illustrated in Figure 16B. The final concentration of probe 1 and Ag^{+} was kept constant at 100 μM, whereas the molar fraction of probe 1 was varied gradually. The fluorescence emission bands for the probe 1:Ag^{+} complex exhibited a maximum of around 0.65 mole fractions of Ag^{+} to receptor 1. Job's plot revealed a 1:2 stoichiometry for the compound. The stoichiometry of the complex between probe 1 and Hg^{2+} ion was determined using Job's plot from emission titration experiments, which is shown in Figure 16A; it demonstrated a maximum for the fluorescence emission bands of about 0.3 mole fractions of Hg^{2+} to probe 1. Job's plot suggested that the stoichiometry of the complex was 2:1.

3.9.7. Probe Quantum Yields (Φ_F). Using quinine sulfate (Φ_F =0.54) as a reference, the fluorescence quantum yield (Φ_F) of the probes in the absence of Hg(II) and Ag(I) ions was calculated. Eq 4 was used to calculate the value of F:

$$\Phi_F = \Phi_{ref} X\, I_{probe}/I_{ref.} X\, A_{ref}/A_{probe}\, X \eta_{probe}^{\ 2}/\eta_{ref.}^{\ 2} \quad (4)$$

where Φ_F and Φ_{ref} are the quantum yields of the probe and quinine sulfate, respectively. I_{probe} and I_{ref} are the integrated emission peak areas of the probe and quinine sulfate, respectively; A_{probe} and A_{ref} are the absorbances of the probe and quinine sulfate at the excitation wavelengths, respectively; η_{probe} and η_{ref} are the refractive indices of solvents, respectively (Figure 17).

4. CONCLUSIONS

In summary, we designed, synthesized, and completely characterized a TPE-based novel probe 1 known as TPE-PVA having a quantum yield (Φ) of 2.26 with AIE (aggregation-induced emission) activity and a remarkable mechanochromic photophysical phenomenon that was studied through grinding, fuming, and heating. The mechanochromic luminescence characteristics were generated by the transition from the crystalline to the amorphous state. The synthesized probe 1 was effective in metal ion sensing in mixed aqueous media and was used as a fluorescent sensor to detect Hg^{2+} and

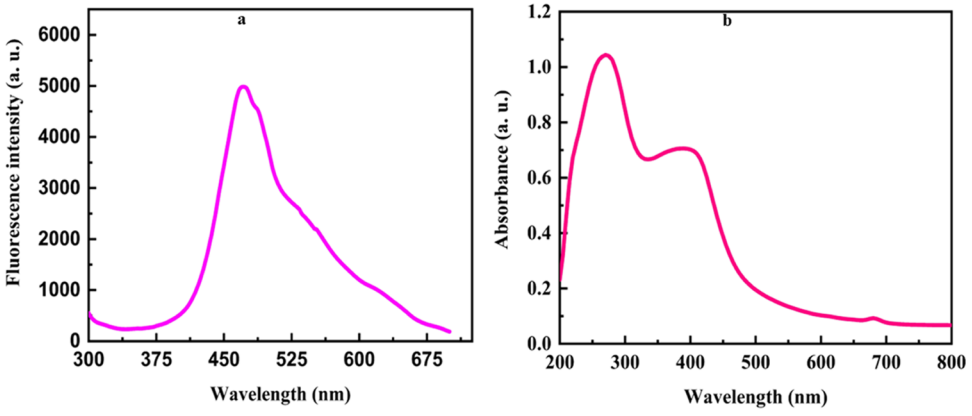

Figure 17. Solid-state spectra of probe 1: (a) emission spectra and (b) excitation spectra.

https://doi.org/10.1021/acsomega.2c03437
ACS Omega 2022, 7, 34888−34900

Ag^+ selectively and sensitively from a mixed aqueous medium (ACN:H_2O, 1:9) over other metal ions. The addition of only Hg^{2+} and Ag^+ significantly turned off the fluorescence of probe 1. The approach was developed to detect both ions selectively using a single probe based on these quenching characteristics. In addition to paper strip-based sensing, the onsite detection of Hg^{2+} and Ag^+ in real samples was performed. Because of the selectivity and sensitivity of probe 1 toward Hg^{2+} and Ag^+ ions as a paper strip sensor, kits for the detection of Hg^{2+} and Ag^+ ions could be developed in the future.

■ ASSOCIATED CONTENT

Supporting Information

The Supporting Information is available free of charge at https://pubs.acs.org/doi/10.1021/acsomega.2c03437.

Proposed binding mode of probe 1 (TPE-PVA) toward Hg^{2+} and Ag^+ analytes; IR spectra of 4-(1,2,2-triphenylvinyl) benzaldehyde (TPE-CHO); ^1H NMR spectra of 4-(1,2,2-triphenylvinyl) benzaldehyde; ^{13}C NMR spectra of 4-(1,2,2-triphenylvinyl) benzaldehyde; HRMS spectra of 4-(1,2,2-triphenylvinyl) benzaldehyde; IR spectra of (*E*)-*N*-methyl-2-(4-(1,2,2-triphenylvinyl) benzylidene) hydrazinecarbothioamide (TPE-PVA); ^1H NMR spectra of (*E*)-*N*-methyl-2-(4-(1,2,2-triphenylvinyl) benzylidene) hydrazinecarbothioamide; ^{13}C NMR spectra of (*E*)-*N*-methyl-2-(4-(1,2,2-triphenylvinyl)-benzylidene) hydrazinecarbothioamide; HRMS spectra of (*E*)-*N*-methyl-2-(4-(1,2,2-triphenylvinyl) benzylidene) hydrazinecarbothioamide (PDF)

■ AUTHOR INFORMATION

Corresponding Author

Prashant V. Anbhule − *Medicinal Chemistry Research Laboratory, Department of Chemistry, Shivaji University, Kolhapur, Maharashtra 416004, India;* orcid.org/0000-0003-1681-6349; Phone: +91 231 260 9169; Email: pvanbhule@gmail.com; Fax: +91 231 2692333

Authors

Kishor S. Jagadhane − *Medicinal Chemistry Research Laboratory, Department of Chemistry, Shivaji University, Kolhapur, Maharashtra 416004, India*

Sneha R. Bhosale − *Medicinal Chemistry Research Laboratory, Department of Chemistry, Shivaji University, Kolhapur, Maharashtra 416004, India*

Datta B. Gunjal − *Fluorescence Spectroscopy Research Laboratory, Department of Chemistry, Shivaji University, Kolhapur, Maharashtra 416004, India*

Omkar S. Nille − *Fluorescence Spectroscopy Research Laboratory, Department of Chemistry, Shivaji University, Kolhapur, Maharashtra 416004, India*

Govind B. Kolekar − *Fluorescence Spectroscopy Research Laboratory, Department of Chemistry, Shivaji University, Kolhapur, Maharashtra 416004, India*

Sanjay S. Kolekar − *Analytical Chemistry and Material Science Research Laboratory, Department of Chemistry, Shivaji University, Kolhapur, Maharashtra 416004, India*

Tukaram D. Dongale − *Computational Electronics and Nanoscience Research Laboratory, School of Nanoscience and Biotechnology, Shivaji University, Kolhapur, Maharashtra 416004, India;* orcid.org/0000-0003-2536-6132

Complete contact information is available at: https://pubs.acs.org/10.1021/acsomega.2c03437

Notes

The authors declare no competing financial interest.

K.S.J. and P.V.A. confirmed that they have no conflicts of interest in this study. The authors declare that they have neither commercial nor associative interests in connection with this research submitted that might cause a conflict of interest.

■ ACKNOWLEDGMENTS

K.S.J. and P.V.A. are thankful to the Department of Chemistry, Shivaji University, Kolhapur, for providing all research facilities, and they are grateful for financial support from Dr. Babasaheb Ambedkar Research and Training Institute (BARTI), Pune (No. BARTI/Fellowship/BANRF-2018/19-20/3036).

■ REFERENCES

(1) Zhu, C.; Kwok, R. T. K.; Lam, J. W. Y.; Tang, B. Z. Aggregation-Induced Emission: A Trailblazing Journey to the Field of Biomedicine. *ACS Appl. Bio Mater.* **2018**, *1*, 1768−1786.

(2) Suman, G. R.; Pandey, M.; Chakravarthy, A. S. J. Review on New Horizons of Aggregation Induced Emission: From Design to Development. *Mater. Chem. Front.* **2021**, 1541−1584.

(3) Hong, Y.; Lam, J. W. Y.; Tang, B. Z. Aggregation-Induced Emission. *Chem. Soc. Rev.* **2011**, *40*, 5361−5388.

(4) Mei, J.; Leung, N. L. C.; Kwok, R. T. K.; Lam, J. W. Y.; Tang, B. Z. Aggregation-Induced Emission: Together We Shine, United We Soar! *Chem. Rev.* **2015**, 11718−11940.

(5) Ishiwari, F.; Hasebe, H.; Matsumura, S.; Hajjaj, F.; Horii-Hayashi, N.; Nishi, M.; Someya, T.; Fukushima, T. Bioinspired Design of a Polymer Gel Sensor for the Realization of Extracellular Ca2+ Imaging. *Sci. Rep.* **2016**, *6*, No. 24275.

(6) La, D. D.; Bhosale, S. V.; Jones, L. A.; Bhosale, S. V. Tetraphenylethylene-Based AIE-Active Probes for Sensing Applications. *ACS Appl. Mater. Interfaces* **2018**, *10*, 12189−12216.

(7) Gao, M.; Tang, B. Z. Fluorescent Sensors Based on Aggregation-Induced Emission: Recent Advances and Perspectives. *ACS Sens.* **2017**, *2*, 1382−1399.

(8) Sharma, R.; Haldar, U.; Turabee, M. H.; Lee, H. i. Recyclable Macromolecular Thermogels for Hg(II) Detection and Separation via Sol-Gel Transition in Complex Aqueous Environments. *J. Hazard. Mater.* **2021**, *410*, No. 124625.

(9) Nadimetla, D. N.; Bhosale, S. V. Tetraphenylethylene AIEgen Bearing Thiophenylbipyridine Receptor for Selective Detection of Copper (Ii) Ion. *New J. Chem.* **2021**, *45*, 7614−7621.

(10) Feng, J.; Yao, L.; Zhang, J.; Mu, Y.; Chi, Z.; Su, C. Y. A Luminescent Silver-Phosphine Tetragonal Cage Based on Tetraphenylethylene. *Dalton Trans.* **2016**, *45*, 1668−1673.

(11) Ruan, Z.; Shan, Y.; Gong, Y.; Wang, C.; Ye, F.; Qiu, Y.; Liang, Z.; Li, Z. Novel AIE-Active Ratiometric Fluorescent Probes for Mercury (II) Based on the Hg2+-Promoted Deprotection of Thioketal, and Good Mechanochromic Properties. *J. Mater. Chem. C* **2018**, *6*, 773−780.

(12) Haldar, U.; Lee, H.-i. BODIPY-Derived Multi-Channel Polymeric Chemosensor with PH-Tunable Sensitivity: Selective Colorimetric and Fluorimetric Detection of Hg2+ and HSO4- in Aqueous Media. *Polym. Chem.* **2018**, *9*, 4882−4890.

(13) Chatterjee, A.; Banerjee, M.; Khandare, D. G.; Gawas, R. U.; Mascarenhas, S. C.; Ganguly, A.; Gupta, R.; Joshi, H. Aggregation-Induced Emission-Based Chemodosimeter Approach for Selective Sensing and Imaging of Hg (II) and Methylmercury Species. *Anal. Chem.* **2017**, *89*, 12698−12704.

(14) Gui, S.; Huang, Y.; Hu, F.; Jin, Y.; Zhang, G.; Zhang, D.; Zhao, R. Bioinspired Peptide for Imaging Hg2+ Distribution in Living Cells and Zebrafish Based on Coordination-Mediated Supramolecular Assembling. *Anal. Chem.* **2018**, *90*, 9708−9715.

(15) Neupane, L. N.; Oh, E. T.; Park, H. J.; Lee, K. H. Selective and Sensitive Detection of Heavy Metal Ions in 100% Aqueous Solution and Cells with a Fluorescence Chemosensor Based on Peptide Using Aggregation-Induced Emission. *Anal. Chem.* **2016**, *88*, 3333−3340.
(16) Cheng, H. B.; Li, Z.; Huang, Y. D.; Liu, L.; Wu, H. C. Pillararene-Based Aggregation-Induced-Emission-Active Supramolecular System for Simultaneous Detection and Removal of Mercury(II) in Water. *ACS Appl. Mater. Interfaces* **2017**, *9*, 11889−11894.
(17) Swamy P, C. A.; Shanmugapriya, J.; Singaravadivel, S.; Sivaraman, G.; Chellappa, D. Anthracene-Based Highly Selective and Sensitive Fluorescent " Turn-on" Chemodosimeter for Hg2+. *ACS Omega* **2018**, *3*, 12341−12348.
(18) Dai, D.; Li, Z.; Yang, J.; Wang, C.; Wu, J. R.; Wang, Y.; Zhang, D.; Yang, Y. W. Supramolecular Assembly-Induced Emission Enhancement for Efficient Mercury(II) Detection and Removal. *J. Am. Chem. Soc.* **2019**, *141*, 4756−4763.
(19) Yuan, B.; Wang, D. X.; Zhu, L. N.; Lan, Y. L.; Cheng, M.; Zhang, L. M.; Chu, J. Q.; Li, X. Z.; Kong, D. M. Dinuclear HgII Tetracarbene Complex-Triggered Aggregation-Induced Emission for Rapid and Selective Sensing of Hg2+ and Organomercury Species. *Chem. Sci.* **2019**, *10*, 4220−4226.
(20) Gao, Z.; Liu, G. G.; Ye, H.; Rauschendorfer, R.; Tang, D.; Xia, X. Facile Colorimetric Detection of Silver Ions with Picomolar Sensitivity. *Anal. Chem.* **2017**, *89*, 3622−3629.
(21) Umar, S.; Jha, A. K.; Purohit, D.; Goel, A. A Tetraphenylethene-Naphthyridine-Based AIEgen TPEN with Dual Mechanochromic and Chemosensing Properties. *J. Org. Chem.* **2017**, *82*, 4766−4773.
(22) Wei, G.; Jiang, Y.; Wang, F. A Novel AIEE Polymer Sensor for Detection of Hg2+ and Ag+ in Aqueous Solution. *J. Photochem. Photobiol., A* **2018**, *358*, 38−43.
(23) Singh, G.; Singh, A.; Satija, P.; Sharma, G.; Shilpy; Singh, J.; Singh, J.; Singh, K. N.; Kaur, A. First Report of Silver Ion Recognition via a Silatrane-Based Receptor: Excellent Selectivity, Low Detection Limit and Good Applicability. *New J. Chem.* **2019**, *43*, 5525−5530.
(24) Liu, L.; Zhang, G.; Xiang, J.; Zhang, D.; Zhu, D. Fluorescence "Turn on" Chemosensors for Ag+ and Hg2+ Based on Tetraphenylethylene Motif Featuring Adenine and Thymine Moieties. *Org. Lett.* **2008**, *10*, 4581−4584.
(25) Haldar, U.; Lee, H.-i. BODIPY-Derived Polymeric Chemosensor Appended with Thiosemicarbazone Units for the Simultaneous Detection and Separation of Hg(II) Ions in Pure Aqueous Media. *ACS Appl. Mater. Interfaces* **2019**, *11*, 13685−13693.
(26) Qayyum, M.; Bushra, T.; Khan, Z. A.; Gul, H.; Majeed, S.; Yu, C.; Farooq, U.; Shaikh, A. J.; Shahzad, S. A. Synthesis and Tetraphenylethylene-Based Aggregation-Induced Emission Probe for Rapid Detection of Nitroaromatic Compounds in Aqueous Media. *ACS Omega* **2021**, *6*, 25447−25460.
(27) Zhao, X.; Ji, C.; Ma, L.; Wu, Z.; Cheng, W.; Yin, M. An Aggregation-Induced Emission-Based "Turn-On" Fluorescent Probe for Facile Detection of Gaseous Formaldehyde. *ACS Sens.* **2018**, *3*, 2112−2117.
(28) Xiang, X.; Zhan, Y.; Yang, W. Tetraphenylethene Functionalized Quinoxaline Derivative Exhibiting Aggregation-Induced Emission and Multi-Stimuli Responsive Fluorescent Switching. *Tetrahedron* **2022**, *104*, No. 132600.
(29) Li, Y.; Li, Y.; Feng, Z.; Peng, Q.; Yang, C.; He, J.; Hu, Q.; Li, K. An AIEgen-Based Luminescent Photo-Responsive System Used as Concealed Anti-Counterfeit Material. *J. Lumin.* **2019**, *216*, No. 116750.
(30) He, Z.; Ke, C.; Tang, B. Z. Journey of Aggregation-Induced Emission Research. *ACS Omega* **2018**, *3*, 3267−3277.
(31) Rodrigues, A. C. B.; Pina, J.; Dong, W.; Forster, M.; Scherf, U.; de Melo, J. S. S. Aggregation-Induced Emission in Phenothiazine-TPE and -TPAN Polymers. *Macromolecules* **2018**, *51*, 8501−8512.
(32) Du, W.; Liu, X.; Liu, L.; Lam, J. W. Y.; Tang, B. Z. Photoresponsive Polymers with Aggregation-Induced Emission. *ACS Appl. Polym. Mater.* **2021**, *3*, 2290−2309.
(33) Siddharth, K.; Alam, P.; Hossain, M. D.; Xie, N.; Nambafu, G. S.; Rehman, F.; Lam, J. W. Y.; Chen, G.; Cheng, J.; Luo, Z.; Chen, G.; Tang, B. Z.; Shao, M. Hydrazine Detection during Ammonia Electro-Oxidation Using an Aggregation-Induced Emission Dye. *J. Am. Chem. Soc.* **2021**, *143*, 2433−2440.
(34) Li, Y.; Dong, Y.; Cheng, L.; Qin, C.; Nian, H.; Zhang, H.; Yu, Y.; Cao, L. Aggregation-Induced Emission and Light-Harvesting Function of Tetraphenylethene-Based Tetracationic Dicyclophane. *J. Am. Chem. Soc.* **2019**, *141*, 8412−8415.
(35) Wang, D.; Qian, J.; Qin, W.; Qin, A.; Tang, B. Z.; He, S. Biocompatible and Photostable AIE Dots with Red Emission for in Vivo Two-Photon Bioimaging. *Sci. Rep.* **2015**, *4*, No. 4279.
(36) Chen, Y.; Lam, J. W. Y.; Kwok, R. T. K.; Liu, B.; Tang, B. Z. Aggregation-Induced Emission: Fundamental Understanding and Future Developments. *Mater. Horiz.* **2019**, *6*, 428−433.
(37) Hong, Y.; Lam, J. W. Y.; Tang, B. Z. Aggregation-Induced Emission: Phenomenon, Mechanism and Applications. *Chem. Commun.* **2009**, 4332−4353.
(38) Zalmi, G. A.; Nadimetla, D. N.; Kotharkar, P.; Puyad, A. L.; Kowshik, M.; Bhosale, S. V. Aggregation-Induced Emission-Based Material for Selective and Sensitive Recognition of Cyanide Anions in Solution and Biological Assays. *ACS Omega* **2021**, *6*, 16704−16713.
(39) Wang, D.; Tang, B. Z. Aggregation-Induced Emission Luminogens for Activity-Based Sensing. *Acc. Chem. Res.* **2019**, *52*, 2559−2570.
(40) Mahendran, V.; Pasumpon, K.; Thimmarayaperumal, S.; Thilagar, P.; Shanmugam, S. Tetraphenylethene-2-Pyrone Conjugate: Aggregation-Induced Emission Study and Explosives Sensor. *J. Org. Chem.* **2016**, *81*, 3597−3602.
(41) Dong, Y. Q.; Lam, J. W. Y.; Tang, B. Z. Mechanochromic Luminescence of Aggregation-Induced Emission Luminogens. *J. Phys. Chem. Lett.* **2015**, *6*, 3429−3436.
(42) Zhang, Y.; Xiong, T.; Möslein, A. F.; Mollick, S.; Kachwal, V.; Babal, A. S.; Amin, N.; Tan, J.-C. Nanoconfinement of tetraphenylethylene in zeolitic metal-organic framework for turn-on mechanofluorochromic stress sensing. *Appl. Mater. Today* **2022**, *27*, No. 101434.
(43) Feng, N.; Gao, C.; Guo, C. Y.; Chen, G. Copper-Phenylacetylide Nanobelt/Single-Walled Carbon Nanotube Composites: Mechanochromic Luminescence Phenomenon and Thermoelectric Performance. *ACS Appl. Mater. Interfaces* **2018**, *10*, 5603−5608.
(44) Benito, Q.; le Goff, X. F.; Maron, S.; Fargues, A.; Garcia, A.; Martineau, C.; Taulelle, F.; Kahlal, S.; Gacoin, T.; Boilot, J. P.; Perruchas, S. Polymorphic Copper Iodide Clusters: Insights into the Mechanochromic Luminescence Properties. *J. Am. Chem. Soc.* **2014**, *136*, 11311−11320.
(45) Yin, Y.; Chen, Z.; Fan, C.; Liu, G.; Pu, S. 1,8-Naphthalimide-Based Highly Emissive Luminophors with Various Mechanofluorochromism and Aggregation-Induced Characteristics. *ACS Omega* **2019**, *4*, 14324−14332.
(46) *INTERNATIONAL CONFERENCE ON HARMONISATION OF TECHNICAL REQUIREMENTS FOR REGISTRATION OF PHARMACEUTICALS FOR HUMAN USE ICH HARMONISED TRIPARTITE GUIDELINE VALIDATION OF ANALYTICAL PROCEDURES: TEXT AND METHODOLOGY Q2(R1)*.
(47) Song, I. H.; Torawane, P.; Lee, J. S.; Warkad, S. D.; Borase, A.; Sahoo, S. K.; Nimse, S. B.; Kuwar, A. The Detection of Al3+and Cu2+ions Using Isonicotinohydrazide-Based Chemosensors and Their Application to Live-Cell Imaging. *Mater. Adv.* **2021**, *2*, 6306−6314.
(48) Chang, M. J.; Kim, K.; Kang, C.; Lee, M. H. Enhanced Aggregability of AIE-Based Probe through H 2 S-Selective Triggered Dimerization and Its Applications to Biological Systems. *ACS Omega* **2019**, *4*, 7176−7181.
(49) Jung, M. J.; Kim, S. J.; Lee, M. H. ∝-Extended Tetraphenylethylene Containing a Dicyanovinyl Group as an Ideal Fluorescence Turn-On and Naked-Eye Color Change Probe for Hydrazine Detection. *ACS Omega* **2020**, *5*, 28369−28374.

https://doi.org/10.1021/acsomega.2c03437
ACS Omega 2022, 7, 34888−34900